Macromolecules **2007,** *40,* 693−702

Supramolecular Diblock Copolymers: A Field-Theoretic Model and Mean-Field Solution

Edward H. Feng*

College of Chemistry, University of California, Berkeley, California 94720

Won Bo Lee and Glenn H. Fredrickson

Materials Research Laboratory, University of California, Santa Barbara, California 93106

Received July 21, 2006; Revised Manuscript Received September 6, 2006

ABSTRACT: We consider a supramolecular diblock copolymer melt in which two homopolymers of different species can reversibly bond at terminal binding sites to form a diblock copolymer. The grand canonical ensemble is particularly convenient for formulating field-theoretic models of supramolecular assembly because the chemical equilibrium of bonding reactions impose constraints on the chemical potentials of the polymer species. Unlike the analogous model for a three component blend of A and B homopolymers with an irreversibly bonded AB diblock copolymer, both χN and N appear as independent parameters, where χ is the Flory interaction parameter and N is the length of the diblock copolymer. In addition, an extra parameter characterizes the free energy of forming a bond. Analytic methods and numerical self-consistent field theory are used to calculate the phase diagram in the mean-field approximation. For symmetric systems with equal volume fractions and chain lengths of the two homopolymers, we predict re-entrant behavior upon cooling in narrow parameter ranges for both disordered and lamellar phases. In the case of the lamellar phase, we find re-entrant behavior in which the intermediate phase is either disordered or macrophase separated. We explain this behavior as a competition between the bonding equilibrium, the chemical incompatibility of the two species and the translational entropy loss upon forming a diblock copolymer.

1. Introduction

Supramolecular polymer systems consist of polymers with one or more bonding groups that can each form a reversible linkage of precise functionality with another bonding group. For example, Sijbesma, Meijer, and co-workers synthesized short telechelic polymers capped on each end with a bonding group.[1] In solution, these polymers bonded together to form long linear supramolecular chains. The reversible nature of the bonding reaction implies that temperature can be used to control the average length of the supramolecular polymers and hence bulk solution properties such as the viscosity. While Meijer's group used reversibly bonding units possessing four adjacent hydrogen bonds, other routes to supramolecular polymers have employed a single hydrogen bond coupled with an ionic interaction,[2] metal ligand complexes,[3] DNA base pairing,[4] and host−guest interactions[5] as the reversible bond. Moreover, this assortment of bonding groups has allowed researchers to use two distinct, noninteracting bonding groups in the same polymer system as an "orthogonal" approach to new materials.[6] Potential applications for these materials include biosensors and light harvesting complexes for solar cells.

We are primarily interested in multicomponent supramolecular polymer systems capable of forming *inhomogeneous* phases. The work of Ruokolainen et al. exemplifies both the interesting physics and the potential applications of inhomogeneous supramolecular polymers.[2] First, they synthesized a graft copolymer system in which end-functionalized A polymers could reversibly bond anywhere along the backbone of B polymers. This system exhibited re-entrant behavior, as they observed transitions from a two phase macrophase separated region to a one phase disordered region and back to a two phase region as temperature increased. Then they replaced the B polymer with a BC diblock copolymer in which the A polymers could only graft to the B block, and this three-component system formed both lamellar and cylindrical morphologies. Moreover, the electrical conductivity of this material showed a large peak as a function of temperature due to the changing morphology, another example of the ability to control material properties with temperature. While this system employed a single hydrogen bond with an ionic interaction as the reversible bond, other examples of inhomogeneous supramolecular polymers have used metal ligand complexes[3] and a series of four adjacent hydrogen bonds.[7]

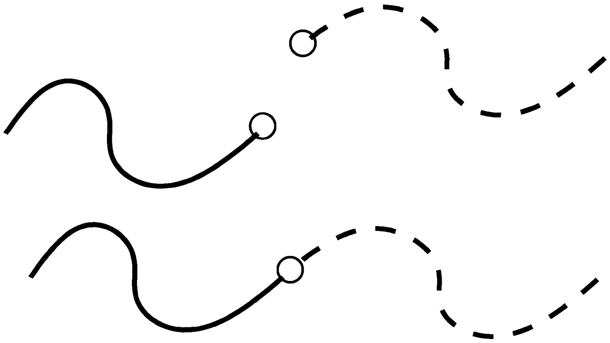

Figure 1. Supramolecular diblock copolymer system in which terminal hetero-complementary bonding groups on A and B homopolymers can reversibly bind to form an AB diblock copolymer.

Because of the large parameter space that characterizes the polymer architectures and molecular weights, chemical incompatibilities of different species and bonding strengths possible in multicomponent supramolecular polymer systems, theory will undoubtedly play an important role in designing these materials. Tanaka and co-workers pioneered this effort by considering A and B homopolymers that could form a diblock copolymer,[8] the system illustrated in Figure 1. They used the random phase

10.1021/ma061653o CCC: $37.00

approximation to study microphase and macrophase separation transitions in this system of supramolecular diblock copolymers (SDC). Subsequent work by the same group employed similar theoretical methods to investigate the two component graft copolymer system studied experimentally by Ruokolainen and co-workers.[9] The group of ten Brinke employed Monte Carlo simulations to study the inhomogeneous phase behavior of supramolecular diblock copolymers[10] and graft copolymers.[11] More recent work by ten Brinke and co-workers has advanced the theoretical methods in analyzing graft and diblock copolymer systems in the weak segregation regime.[12]

Despite the success of this theoretical work, it is desirable to go beyond the weak segregation regime and apply numerical self-consistent field theory (SCFT) to investigate supramolecular polymers at arbitrary segregation strengths. The formalism of ten Brinke and co-workers, which is framed in the canonical ensemble and imposes binding equilibrium using an approximation that deteriorates at higher segregation strength, is not easily extended to numerical SCFT. Therefore, an important aspect of the present paper is recasting the field-theoretic description of supramolecular polymers into a form where the conditions of bonding equilibrium are exact at all segregation strengths. This versatile framework can be used to investigate the self-assembly of broad classes of inhomogeneous supramolecular polymers. While the mean-field approximation (SCFT) is applied in the present work, we emphasize that our theoretical framework does not rely on this approximation and more general field-theoretic simulation techniques[13,14] could be applied.

Here we consider a SDC model in which reversible bonds only result in diblock copolymers, the situation depicted in Figure 1. This case of *hetero-complementary* binding occurs experimentally when the bonding groups on the A homopolymers can only bind to the groups on the B homopolymers. It is straightforward to generalize to the case in which one or both homopolymers have *self-complementary* bonding groups so that pairs of homopolymers can link together. We formulate our SDC model in the grand canonical ensemble, the most natural way to describe a chemically reacting system. The model employs continuous Gaussian chains, characterizes the chemical incompatibility of the two species with a Flory−Huggins parameter χ and prescribes a free energy change upon linking A and B homopolymers to form a diblock copolymer. Our numerical results for a symmetric system with A and B homopolymers of the same length and volume fraction show inhomogeneous re-entrant behavior in which a lamellar phase disappears with decreasing temperature but then reappears at a lower temperature.

This paper has the following organization. Section 2 formulates the field-theoretic model in the grand canonical ensemble. We outline our methods for calculating phase diagrams in section 3, while section 4 displays the resulting phase diagrams and discusses the re-entrant behavior. We conclude in section 5 by discussing the relationship of this theoretical work with experiments.

2. Model Development

Our supramolecular diblock copolymers (SDC) model consists of an incompressible melt of n_K^0 original homopolymers of length N_K for K = A, B contained within a volume V. The hetero-complementary bonding groups at one end of each A and B homopolymer allow two homopolymers of different species to form an AB diblock copolymer of length $N \equiv N_A + N_B$. The generalization of our formalism to self-complementary bonding groups is straightforward. The chemical equilibrium for this bonding reaction determines n_{AB}, the number of diblock copolymers. Our coarse grained model for this reaction assumes a free energy change F_b upon forming a diblock copolymer that accounts for the microscopic details of joining two terminal bonding groups. In general, F_b has an energetic and entropic contribution, and we emphasize that F_b only reflects the formation free energy of a bond between two functional groups in close proximity. Larger scale energetic and entropic effects associated with, e.g., differences in conformational properties and translational entropies of reactants (homopolymers) and products (diblocks) are explicitly accounted for in the model. For simplicity, we express F_b and all subsequent energies in units of kT.

We assume flexible polymers and apply a continuous Gaussian chain model so that $\mathbf{R}_{iK}(s)$ denotes a contour point $s \in [0, N_K]$ on a space curve $\mathbf{R}_{iK}$ for chain $i = 1, 2, ..., n_K^0$ of species K = A, B. The harmonic stretching energy for one polymer chain is

$$U_0[\mathbf{R}_{iK}] = \frac{3}{2b^2}\int_0^{N_K}\left|\frac{d\mathbf{R}_{iK}(s)}{ds}\right|^2 ds \qquad (1)$$

where b is the statistical segment length, taken to be the same for both polymer species. The total stretching energy for this system (prior to allowing any reaction) is

$$U_0[\mathbf{R}_A, \mathbf{R}_B] = \sum_{K=A,B}\sum_{i=1}^{n_K^0} U_0[\mathbf{R}_{iK}] \qquad (2)$$

where $\mathbf{R}_K$ for K = A, B denotes the set of space curves $\mathbf{R}_{iK}$ for $i = 1...n_K^0$. We model attractive interactions among segments of the same species through the quadratic interaction

$$U_1[\mathbf{R}_A, \mathbf{R}_B] = v_0\chi\int \hat{\rho}_A(\mathbf{r})\hat{\rho}_B(\mathbf{r})\, d\mathbf{r} \qquad (3)$$

where χ is the A−B Flory interaction parameter, microscopic segment densities are defined by $\hat{\rho}_K(\mathbf{r}) = \sum_{i=1}^{n_K^0}\int_0^{N_K}\delta(\mathbf{r} - \mathbf{R}_{iK}(s))\, ds$ and v_0 is a common segment volume for both species. To capture repulsive interactions among polymer segments, we assume incompressible melt conditions which fixes the density at $\rho_0 = \hat{\rho}_A(\mathbf{r}) + \hat{\rho}_B(\mathbf{r}) = v_0^{-1}$ for each point $\mathbf{r}$.

We formulate the equilibrium statistical mechanics of this model in the grand canonical ensemble for fixed activity of the A homopolymer z_A, volume V, and temperature T. The activity z_B of the B homopolymer does not appear as an independent parameter because the incompressibility constraint fixes the total number of segments in the system. Moreover, no independent activity z_{AB} is present for the diblock species because, as discussed further below, reaction equilibrium provides an independent condition that relates the chemical potentials (and thus activities) of the reactants and products. The detailed description of the model and conversion to field-theoretic form by means of a Hubbard−Stratonovich−Edwards transformation are given in Appendix A.1. The grand canonical partition function

$$\Xi(z_A, V, T) = \int \mathscr{D}W_\pm\, e^{-\mathscr{H}[W_\pm]} \qquad (4)$$

is expressed as a functional integral over fields $W_\pm(\mathbf{x})$, which denote fluctuating potential fields $W_+(\mathbf{x})$ and $W_-(\mathbf{x})$ conjugate to the linear combination of densities $(\rho_A(\mathbf{x}) + \rho_B(\mathbf{x}))/N$ and $(\rho_A(\mathbf{x}) - \rho_B(\mathbf{x}))/N$ respectively. The effective Hamiltonian is

$$\frac{\mathscr{H}[W_\pm]N}{\rho_0 V} = \frac{1}{\chi N \bar{V}}\int W_-(\mathbf{x})^2\,\mathrm{d}\mathbf{x} - \frac{1}{\bar{V}}\int iW_+(\mathbf{x})\,\mathrm{d}\mathbf{x} - z_\mathrm{A}Q_\mathrm{A}[W_\pm] - Q_\mathrm{B}[W_\pm] - z_\mathrm{A}\mathrm{e}^{-F_\mathrm{b}}N^{-1}Q_\mathrm{AB}[W_\pm] \quad (5)$$

where $\bar{V} \equiv V/R_{g0}^3$ and $\mathbf{x} \equiv \mathbf{r}/R_{g0}$ are dimensionless volumes and position vectors in units of $R_{g0} = b(N/6)^{1/2}$, the ideal radius of gyration of a diblock copolymer. The activity of A homopolymers, z_A, has also been nondimensionalized in units of ρ_0/N; this is also done implicitly in previous field-theoretic models of polymer blends.[15] $Q_\mathrm{L}[W_\pm]$ for L = A, B, AB is the normalized single chain partition function for a polymer in the external fields $W_\pm(\mathbf{x})$. For the A species,

$$Q_\mathrm{A}[W_\pm] = \frac{\int \mathscr{D}\mathbf{R}_{1\mathrm{A}}\mathrm{e}^{-U_0[\mathbf{R}_{1\mathrm{A}}] - \int_0^f [iW_+(\mathbf{R}_{1\mathrm{A}}(t)) - W_-(\mathbf{R}_{1\mathrm{A}}(t))]\mathrm{d}t}}{\int \mathscr{D}\mathbf{R}_{1\mathrm{A}}\mathrm{e}^{-U_0[\mathbf{R}_{1\mathrm{A}}]}} \quad (6)$$

where $t = s/N$ and $f \equiv N_\mathrm{A}/N$ is the volume fraction of the A block of each diblock copolymer. Similar expressions can be written for the diblock copolymer and B homopolymer. The factor N^{-1} that multiplies $Q_\mathrm{AB}[W_\pm]$ in eq 5 results from the decreasing number of bonding groups available to form diblock copolymers with increasing N; the concentration of these groups scales as N^{-1} in an incompressible melt. This is a distinguishing feature of chemically reacting systems and leads to a model dependence on both χN and N, unlike the typical case of nonreacting block copolymers and blends.[14] We discuss this point further in section 3 and Appendix A.2.

Since our SDC model involves an incompressible mixture of a block copolymer and two homopolymers, there is a close relationship between the model and standard models for ternary blends of permanently bonded AB diblock copolymer with A and B homopolymer.[16] If we simply replace the factor $z_\mathrm{A}\mathrm{e}^{-F_\mathrm{b}}N^{-1}$ that multiplies Q_AB in eq 5 with an independent diblock copolymer activity z_AB, the grand canonical description of a fixed-bonded ternary blend is immediately recovered. For the SDC model, we can understand the particular expression for z_AB in terms of chemical equilibrium. Specifically, the law of mass action implies that

$$\frac{z_\mathrm{AB}}{z_\mathrm{A}z_\mathrm{B}} = K_\mathrm{eq} = \mathrm{e}^{-F_\mathrm{b} - \ln N} \quad (7)$$

where K_eq is an equilibrium constant for the binding reaction. The factor of ln N in the exponent arises naturally from the aforementioned scaling of the activities by the average chain density ρ_0/N and represents the translational entropy loss upon binding two homopolymers to form a diblock. Since z_A and z_B are not independent parameters in an incompressible model, we are free to set $z_\mathrm{B} = 1$, upon which $z_\mathrm{AB} = z_\mathrm{A}\mathrm{e}^{-F_\mathrm{b}}N^{-1}$ and the prefactor of Q_AB in eq 5 is obtained. At a fundamental level, eq 7 results from the chemical equilibrium condition $\mu_\mathrm{AB} = \mu_\mathrm{A} + \mu_\mathrm{B}$ relating the chemical potentials of reactants and products. Our treatment of reaction equilibria is therefore exact for all values of χN, while previous theoretical treatments are limited to the weak segregation regime.[10−12] More details concerning the treatment of chemical equilibrium are presented in Appendix A.1.

To evaluate the single chain partition functions in eq 5, we introduce a forward propagator $q(\mathbf{x}, t; [W_\pm])$ that satisfies the modified diffusion equation

$$\frac{\partial}{\partial t}q(\mathbf{x}, t; [W_\pm]) = \nabla^2 q(\mathbf{x}, t; [W_\pm]) - \psi(\mathbf{x}, t)q(\mathbf{x}, t; [W_\pm]) \quad (8)$$

with the initial condition $q(\mathbf{x}, 0;[W_\pm]) = 1$ for all $\mathbf{x}$ where

$$\psi(\mathbf{x}, t) = \begin{cases} iW_+(\mathbf{x}) - W_-(\mathbf{x}) & t \in (0, f) \\ iW_+(\mathbf{x}) + W_-(\mathbf{x}) & t \in (f, 1) \end{cases} \quad (9)$$

is the external field. One can show that

$$Q_\mathrm{A}[W_\pm] = \frac{1}{\bar{V}}\int q(\mathbf{x}, f; [W_\pm])\,\mathrm{d}\mathbf{x} \quad (10)$$

$$Q_\mathrm{AB}[W_\pm] = \frac{1}{\bar{V}}\int q(\mathbf{x}, 1; [W_\pm])\,\mathrm{d}\mathbf{x} \quad (11)$$

To calculate $Q_\mathrm{B}[W_\pm]$, we define a backward propagator $q^\dagger(\mathbf{x}, t;[W_\pm])$ that satisfies the diffusion equation

$$\frac{\partial}{\partial t}q^\dagger(\mathbf{x}, t; [W_\pm]) = \nabla^2 q^\dagger(\mathbf{x}, t; [W_\pm]) - \psi^\dagger(\mathbf{x}, t)q^\dagger(\mathbf{x}, t; [W_\pm]) \quad (12)$$

where

$$\psi^\dagger(\mathbf{x}, t) = \begin{cases} iW^{+}(\mathbf{x}) + W_-(\mathbf{x}) & t \in (0, 1 - f) \\ iW_+(\mathbf{x}) - W_-(\mathbf{x}) & t \in (1 - f, 1) \end{cases} \quad (13)$$

with the initial condition $q^\dagger(\mathbf{x}, 0;[W_\pm]) = 1$ for all $\mathbf{x}$. Then

$$Q_\mathrm{B}[W_\pm] = \frac{1}{\bar{V}}\int q^\dagger(\mathbf{x}, 1 - f; [W_\pm])\,\mathrm{d}\mathbf{x} \quad (14)$$

is the single chain partition function for the B homopolymer.

In this paper, we shall focus exclusively on mean-field or saddle point solutions to the above field theoretic model for SDC. One obtains the mean-field equations by requiring that the effective Hamiltonian is stationary with respect to the two fields, i.e.

$$\frac{N}{\rho_0 R_{g0}^3}\frac{\partial\mathscr{H}[W_\pm]}{\partial W_-(\mathbf{x})} = \frac{2}{\chi N}W_-(\mathbf{x}) - \phi_\mathrm{A}(\mathbf{x}; [W_\pm]) + \phi_\mathrm{B}(\mathbf{x}; [W_\pm]) = 0 \quad (15)$$

$$\frac{N}{\rho_0 R_{g0}^3}\frac{\partial\mathscr{H}[W_\pm]}{\partial iW_+(\mathbf{x})} = -1 + \phi_\mathrm{A}(\mathbf{x}; [W_\pm]) + \phi_\mathrm{B}(\mathbf{x}; [W_\pm]) = 0 \quad (16)$$

where the volume fractions of A and B segments are given by

$$\phi_\mathrm{A}(\mathbf{x}; [W_\pm]) = z_\mathrm{A}\int_0^f q(\mathbf{x}, t; [W_\pm])q(\mathbf{x}, f - t; [W_\pm])\,\mathrm{d}t + z_\mathrm{A}\mathrm{e}^{-F_\mathrm{b} - \ln N}\int_0^f q(\mathbf{x}, t; [W_\pm])q^\dagger(\mathbf{x}, 1 - t; [W_\pm])\,\mathrm{d}t \quad (17)$$

$$\phi_\mathrm{B}(\mathbf{x}; [W_\pm]) = \int_0^{1-f} q^\dagger(\mathbf{x}, t; [W_\pm])q^\dagger(\mathbf{x}, 1 - f - t; [W_\pm])\,\mathrm{d}t + z_\mathrm{A}\mathrm{e}^{-F_\mathrm{b} - \ln N}\int_f^1 q(\mathbf{x}, t; [W_\pm])q^\dagger(\mathbf{x}, 1 - t; [W_\pm])\,\mathrm{d}t \quad (18)$$

In these volume fraction expressions, the first and second terms in the sum, respectively, correspond to the contributions from the homopolymers and diblock copolymers. Because of the lengths of the polymers in this reacting system, there is no need to calculate propagators specifically for the A or B homopolymers.

A saddle point solution to the model corresponds to the fields $W_\pm^*(\mathbf{x})$ that satisfy eqs 15 and 16. In general, $W_\pm^*(\mathbf{x})$ are complex valued fields, but we are interested only in physically meaningful fields that lead to real valued $\phi_A(\mathbf{x})$ and $\phi_B(\mathbf{x})$. Equation 15 immediately implies that $W_-^*(\mathbf{x})$ must be real for all $\mathbf{x}$. Moreover, the assumption that $W_+^*(\mathbf{x})$ is purely imaginary leads to real valued $q(\mathbf{x}, t; [W_\pm])$ for all $\mathbf{x}$ and t and hence real valued volume fractions. We define real valued fields $P(\mathbf{x}) \equiv iW_+(\mathbf{x})$ and $E(\mathbf{x}) \equiv W_-(\mathbf{x})$, corresponding to "pressure" and "exchange" potentials, respectively, which reduces the search space for saddle points by a factor of $^1/_2$.

3. Calculating Phase Diagrams

In the present work, we consider a bonding free energy $F_b = -h$ where h is the energy decrease upon forming a diblock copolymer in units of the thermal energy kT. The assumption that the binding is purely energetic implies that $h \sim 1/T$. We note, however, that it may be necessary to include a bonding entropy in F_b to make quantitative comparison with experiments. To calculate a phase diagram for the supramolecular diblock copolymer model, we compare the mean-field free energy given in eq 5 for various ordered and disordered phases at different values of z_A. It is helpful to analytically compute the free energy for the homogeneous disordered phase in which case the fields $E(\mathbf{x}) = E_h$ and $P(\mathbf{x}) = P_h$ are independent of $\mathbf{x}$. This implies

$$\phi_{Ah} = z_A f e^{-(P_h - E_h)f} \tag{19}$$

$$\phi_{Bh} = (1-f)e^{-(P_h+E_h)(1-f)} \tag{20}$$

$$\phi_{AB} = z_A e^{-F_b - \ln N - P_h - (1-2f)E_h} \tag{21}$$

for the volume fraction of the A homopolymer, B homopolymer, and diblock copolymer, respectively. This leads to a homogeneous free energy of

$$\mathscr{F} \equiv \frac{\mathscr{H}[W_\pm^*]N}{\rho_0 V} = \chi N \phi_A(1-\phi_A) + \left(\frac{\phi_A}{f} - \phi_{AB}\right)\left[\ln\left(\frac{\phi_A}{f} - \phi_{AB}\right) - 1\right] + \left(\frac{1-\phi_A}{1-f} - \phi_{AB}\right)\left[\ln\left(\frac{1-\phi_A}{1-f} - \phi_{AB}\right) - 1\right] + \phi_{AB}(\ln \phi_{AB} - 1) - \mu_A \frac{\phi_A}{f} + \phi_{AB}(F_b + \ln N) - \frac{\chi N}{4} \tag{22}$$

and a chemical potential of

$$\mu_A \equiv \ln z_A = \ln\left(\frac{\phi_A}{f} - \phi_{AB}\right) - \frac{f}{1-f}\ln\left(\frac{1-\phi_A}{1-f} - \phi_{AB}\right) - \chi N f\,(2\phi_A - 1)$$

where we choose the total volume fraction of A segments contributed by A homopolymer and diblock, $\phi_A = \phi_{Ah} + f\phi_{AB}$, and the volume fraction of diblock copolymer, ϕ_{AB}, as the two independent compositions in this incompressible system. The free energy in eq 22 has the familiar Flory form with the first four terms after the equality corresponding to the energy and translational entropy of a ternary blend. In addition, the terms $\phi_{AB}F_b$ and $\phi_{AB} \ln N$ represent the local free energy change of the bonding groups and translational entropy loss, respectively, upon forming diblock copolymers in this reacting system. These results are consistent with a Flory lattice treatment for the homogeneous phase of a SDC model[12] where the $\phi_{AB} \ln N$ term arises from the conservation of species in the chemical reaction. However, the final expression given by Angerman and ten Brinke is independent of N due to a compensating $-\ln N$ term in their bonding free energy. Since F_b corresponds to a local interaction of bonding groups whose value should not depend on the molecular weight of the chains to which the groups are attached, we believe that F_b should be independent of N. We discuss these issues further in Appendix A.2.

A "mass action" law for the homogeneous phase follows immediately from eqs 19−21

$$\frac{\phi_{AB}}{[\phi_{Ah}/f][\phi_{Bh}/(1-f)]} = e^{-F_b - \ln N} \tag{23}$$

and expresses the chemical equilibrium of the bonding reaction. It should be emphasized that this formula involving volume fractions holds only for the homogeneous phase, in contrast to the mass action law eq 7 that is exact under all conditions. We use $\phi_{Ah} = \phi_A - f\phi_{AB}$ and $\phi_{Bh} = 1 - \phi_A - (1-f)\phi_{AB}$ to solve eq 23 for ϕ_{AB} as a function of ϕ_A; substituting this result into eq 22 gives the free energy as a function of ϕ_A. We determine phase transitions between disordered and macrophase separated phases from the minima of this free energy.

We first consider the parameters $f = 0.5$ and $z_A = 1$ and study phases with equal numbers of A and B segments, i.e., $\int \phi_A(\mathbf{x})\,d\mathbf{x} = \int \phi_B(\mathbf{x})\,d\mathbf{x}$. This symmetric system is analogous to the isopleth in ternary blend systems,[17] and we expect only homogeneous and lamellar phases. Since the homopolymers are shorter than the diblock copolymer in the SDC model by a factor of 2, previous work on ternary blends suggests the existence of an isotropic Lifshitz point at which disordered, coexisting homogeneous phases, and lamellar regions of the phase diagram meet. For example, a ternary blend of a symmetric diblock copolymer with homopolymers of half the diblock length and a total A volume fraction of 0.5 has a mean-field Lifshitz point located at $\chi N = 6$ and $\phi_{AB} = {}^1/_3$. Exploiting the correspondence between this ternary blend with covalently bonded diblock copolymers and SDC with $f = 0.5$ and $z_A = 1$, we use eqs 19 and 21 to find that $F_b = \ln(4/3N)$ or $h = \ln(3N/4)$ is the condition locating the mean-field Lifshitz point in the SDC model. This result is also obtained by applying the random phase approximation to the SDC model in the grand canonical ensemble; see Appendix A.3 for details of this calculation. It should also be emphasized that an isotropic Lifshitz point is present only in mean field theory. Thermal fluctuations stabilize a bicontinuous microemulsion phase in the region of this point.[18] Nonetheless, the exercise of locating the mean-field Lifshitz point is useful in establishing the topology of the phase diagram as well as parameter values for which bicontinuous morphologies are expected.[19]

We use numerical self-consistent field theory (SCFT) to evaluate the free energies of single unit cells of candidate inhomogeneous phases. This requires finding the inhomogeneous real fields $E^*(\mathbf{x})$ and $P^*(\mathbf{x})$ that satisfy the mean-field eqs 15 and 16. For a particular inhomogeneous phase, we begin with fields possessing the symmetries of the phase and solve the modified diffusion equations in eq 8 and 12 with a pseudospectral algorithm.[14,20] The segment volume fractions in eq 17 and 18 are then evaluated by applying Simpson's rule on a uniform collocation grid, and the fields are updated by a semi-implicit relaxation scheme until an error criterion is satisfied.[14,21,22] We also minimize the free energy with respect to the volume and shape of the periodic simulation box with a variable cell shape method.[14,23] This optimization determines

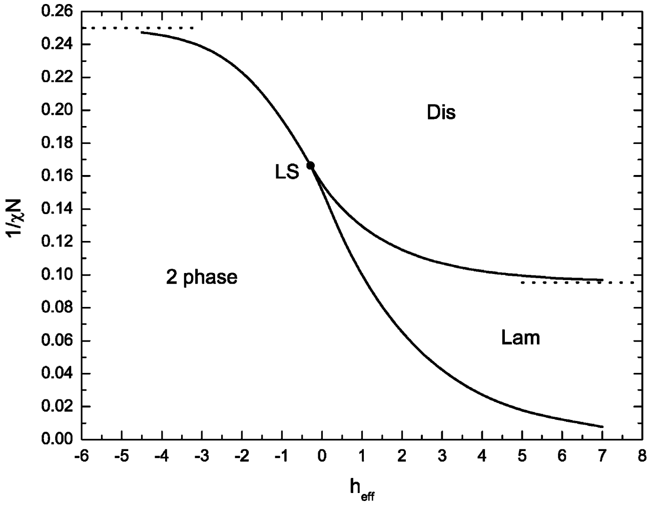

Figure 2. Universal mean-field phase diagram for the supramolecular diblock copolymer model in the coordinates of $h_{\mathrm{eff}} \equiv h - \ln N$ vs $1/(\chi N)$ in the symmetric isopleth plane $z_A/z_B = 1.0$ and $N_A = N_B$. Labeled phases are Dis (homogeneous phase), Lam (lamellar phase) and 2 phase (coexisting A-rich and B-rich homogeneous phases). The solid dot denotes the Lifshitz point (LS). The horizontal dashed line on the left of the diagram denotes $1/\chi N = {}^1/_4$, the macrophase separation transition for a binary blend of polymers. The horizontal dashed line on the right of the diagram signifies $1/\chi N \approx 0.095$, the order−disorder transition for a symmetric diblock copolymer.[24]

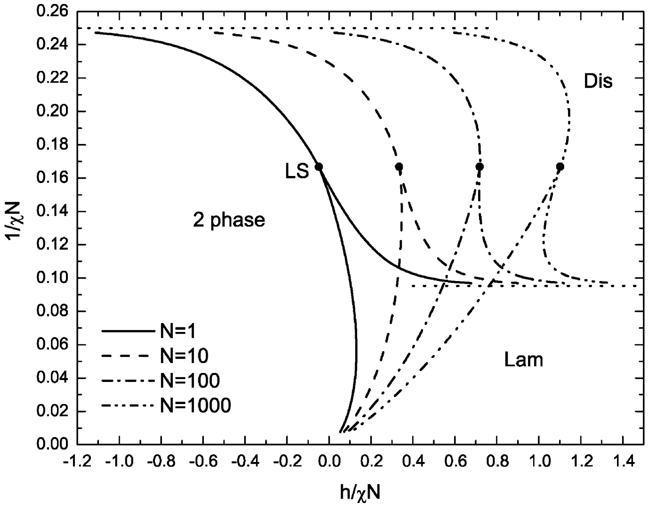

Figure 3. Mean-field phase diagram for the supramolecular diblock copolymer model with $z_A/z_B = 1.0$, and $N_A = N_B$. Labeled phases are Dis (homogeneous disordered phase), Lam (lamellar phase), 2 phase (coexisting A-rich and B-rich homogeneous phases). The values of N indicate the diblock copolymer length. Solid dots denote Lifshitz points (LS). The horizontal dashed line on the left of the diagram denotes $1/\chi N = {}^1/_4$, the macrophase separation transition for a binary blend of polymers. The horizontal dashed line on the right of the diagram signifies $1/\chi N \approx 0.095$, the order−disorder transition for a symmetric diblock copolymer.[24]

the cell volume and shape for which there is no residual internal stress. The minor modifications needed to implement these methods in the grand canonical ensemble are discussed in Appendix A.4. Because we conduct our numerical SCFT calculations in the grand canonical ensemble, the activity z_A and binding energy h are manipulated parameters, while the volume fractions ϕ_A, ϕ_B, and ϕ_{AB} are byproducts of the numerical procedure.

4. Results

We begin by discussing our numerical SCFT results for symmetric supramolecular diblock copolymers (SDC) with equal chain lengths, $N_A = N_B = N/2$ (i.e., $f = 1/2$), and equal volume fractions of A and B homopolymers (set by choosing $z_A = z_B = 1$). In Figure 2 we display a "universal" phase diagram expressed in the coordinates of $1/(\chi N)$ and $h_{\mathrm{eff}} \equiv h - \ln N$. The numerical SCFT calculation confirms the location of the Lifshitz point at $h_{\mathrm{eff}} = \ln(3/4) \approx -0.287$. For $h_{\mathrm{eff}} < \ln(3/4)$, macrophase separation into coexisting A-rich and B-rich homogeneous phases is predicted upon lowering the value of $1/\chi N$. We note that decreasing $1/\chi N$ at fixed h_{eff} does not correspond to decreasing temperature since $h_{\mathrm{eff}} = h - \ln N$ depends on temperature; this issue is addressed in our subsequent phase diagrams. At such weak bonding strengths, the diblock concentration is sufficiently low that microphase separation is not possible. In the asymptotic limit of $h_{\mathrm{eff}} \rightarrow -\infty$, there is strictly no diblock copolymer in the melt, so we recover the binary blend case in which macrophase separation occurs at $1/(\chi N) = {}^1/_4$. As h_{eff} becomes larger than ln(3/4), a lamellar phase emerges, and the range of $1/\chi N$ values in which this phase is stable increases with increasing binding energy h_{eff}. Finally, the limit of a pure symmetric diblock copolymer melt with an order−disorder transition of $1/\chi N \approx 0.095$[24] is attained for $h_{\mathrm{eff}} \rightarrow \infty$.

While Figure 2 highlights the general features of the phase diagram, it does not explicitly show the phase behavior as a function of N, the diblock copolymer length. Moreover, it would be experimentally valuable to have a phase diagram with a clear temperature dependence; this is not the case in Figure 2 as both axes depend on temperature. To accomplish these goals, we note that the three relevant energies are the thermal energy kT, the bonding energy $h(kT)$ and the segment−segment interaction energy $\chi N(kT)$. It proves convenient to scale the thermal and bonding energies by the interaction energy, which implies a dimensionless temperature of $1/\chi N$ and a dimensionless bonding energy of $h/\chi N$. Since we assume that h and χ are purely enthalpic quantities, $h/\chi N$ does not depend on temperature. In Figure 3, we have re-plotted the symmetric phase diagram in the coordinates of $1/\chi N$ vs $h/\chi N$. Each curve corresponds to the indicated value of N, and the curve with $N = 1$ is simply the universal diagram in Figure 2 plotted with a different horizontal axis. Each vertical slice of Figure 3 shows the effect of changing temperature at a fixed ratio of bonding to interaction energy.

Figure 3 shows that the two phase region becomes larger with increasing N. This results from the fact that the concentration of reactants, namely functional end groups, scales as $1/N$, so very few diblocks are formed at large N unless the binding energy is very large. Thus, for increasing N at fixed χN, a larger bonding energy is required to form enough diblock copolymers to induce microphase separation. Perhaps most interesting is that Figure 3 shows *three* distinct types of re-entrant behavior in which a particular phase will disappear with decreasing temperature only to re-appear at a lower temperature. First, the $N = 1000$ case displays a sequence of transitions from lamellar to disordered to lamellar phases with decreasing temperature at $h/\chi N \approx 1.05$. At slightly larger $h/\chi N$ for $N = 1000$, there is re-entrant behavior among homogeneous phases involving transitions from disordered to macrophase separated to disordered phases. Finally, the phase diagrams for $N = 1$ and $N = 10$ show a narrow band of thermally induced transitions from lamellar to macrophase separated to lamellar phases. Homogeneous re-entrant behavior has been predicted for a SDC model previously[12] and is a well-known phenomenon in binary mixtures of low molecular weight associating fluids.[25] Since the re-entrant behavior in binary fluids is understood as a result of hydrogen bonding between molecules of different species, it is not surprising that our SDC model shows the same behavior

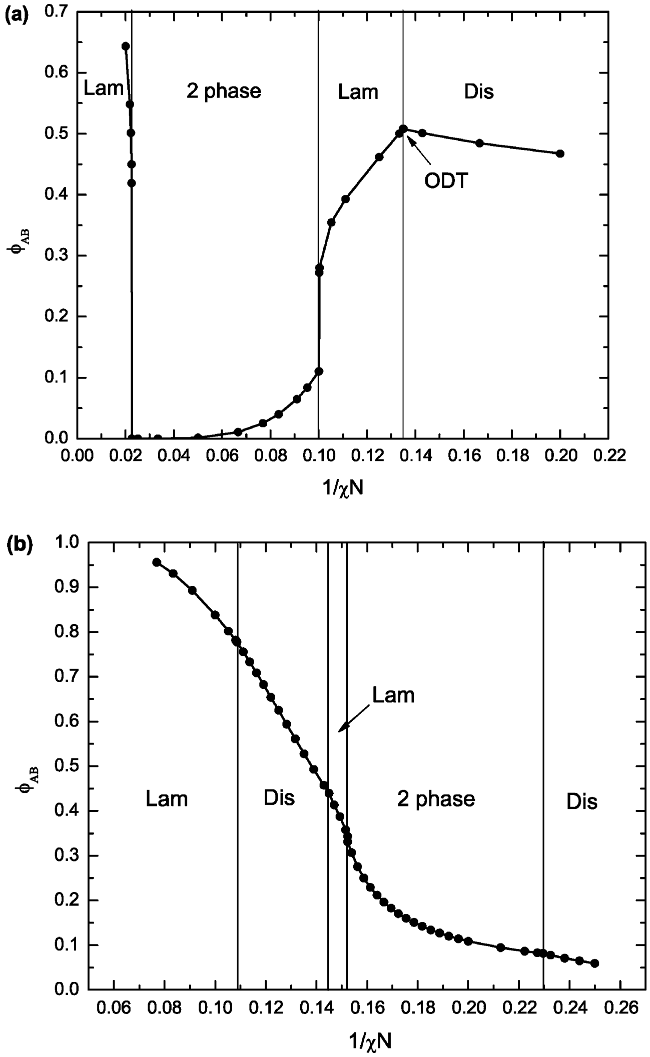

Figure 4. (a) Volume fraction of diblock copolymer for the symmetric SDC model with $h/\chi N = 0.1$ and $N = 1$. (b) Volume fraction of diblock copolymer for the symmetric SDC model with $h/\chi N = 1.05$ and $N = 1000$.

in the homogeneous regime. However, we are unaware of any previous theoretical or experimental work on the re-appearance of an inhomogeneous phase in a supramolecular polymer system.

To better understand the inhomogeneous re-entrant behavior, we consider the competition between three factors. The bonding reaction induces diblock copolymer formation while chemical incompatibility and the translational entropy loss upon forming a diblock copolymer favor homopolymer formation. The effect of these three factors is most clearly seen in the behavior of the diblock copolymer volume fraction as a function of temperature in the re-entrant regime. Figure 4a displays this information for $N = 1$ and a fixed value of $h/\chi N = 0.1$. Starting in the high temperature (large $1/\chi N$) disordered phase, we see that the diblock volume fraction initially rises upon cooling since the binding equilibrium is shifted to more copolymer product. However, once the ODT occurs and a lamellar phase is formed, the microphase separation physically separates the reactants in space, which in turn shifts the equilibrium back to homopolymers. Thus, the diblock fraction decreases with decreasing $1/\chi N$. Eventually there is not enough diblock to maintain the mesophase and the system breaks into two coexisting macrophases to maximize the translational entropy of the polymers. Once this occurs, there is an even more substantial physical separation of homopolymer reactants and the copolymer fraction drops precipitously. Finally, upon cooling to very low temperatures, at which point the importance of translational entropy diminishes, the systems seeks an energy minimum by forming diblock copolymers and hence a lamellar phase. This complicated nonmonotonic behavior of the copolymer volume fraction is apparently a ubiquitous feature of SDC systems at very low molecular weight.

In Figure 4b, we show the behavior of the diblock volume fraction for a more realistic $N = 1000$ case and fixed $h/\chi N = 1.05$. Here, a larger value of $h/\chi N$ is required to overcome the low concentration ($\sim 1/N$) of reactant end groups and produce enough copolymer to form a lamellar phase. In this regime, however, the chemical incompatibility plays a less significant role and the diblock copolymer volume fraction increases monotonically with decreasing temperature. The large bonding energy creates enough copolymer to stabilize against macrophase separation as the temperature is lowered, so the intermediate phase separating the two occurrences of the lamellar phase is disordered. In reality, with thermal fluctuations accounted for, we would expect much of the region surrounding the intermediate disordered phase to be replaced with a bicontinuous microemulsion.

To gain some insight into the asymmetric case when the total volume fractions of A and B polymer segments are not equal, we show the phase diagram for $z_A/z_B = 2$, $f = 0.5$ ($N_A = N_B$), and $N = 100$ in Figure 5, parts a and b. With increasing bonding strength at a fixed temperature $1/\chi N < 0.102$, Figure 5a shows that the system passes through disordered, body-centered cubic spheres (space group $Im\bar{3}m^{II}$), hexagonally packed cylinders, bicontinuous gyroid ($Ia\bar{3}d^{II}$), and lamellar phases. The double diamond phase ($Pn3m^{II}$) is not stable anywhere in the phase diagram. Since $z_A > z_B$, the disordered phase is enriched in the A species. Larger bonding energies favor the formation of diblock copolymers, which pulls more B chains into the system from the reservoir and decreases the total volume fraction of the A species. This is analogous to moving from $f = 1$ to $f = 0.5$ in the ordered region of the diblock copolymer phase diagram,[26] and we observe the same sequence of phases in both diblock copolymers and supramolecular diblock copolymers. Moreover, theoretical studies of ternary blends of A and B homopolymer with symmetric AB diblock copolymer also show the same sequence of phases when increasing the volume fraction of diblock copolymers.[16] In Figure 5b, we superimpose the $z_A = 2$ phase diagram on the $z_A = 1$ diagram, which shows that higher bonding energies are required to access the ordered region in asymmetric systems. While these results shed light on systems with unequal volume fractions of A and B species, it would be difficult to compare the phases diagrams in Figure 5 with experiments since ϕ_A is not constant throughout the diagram.

5. Conclusions and Outlook

In the present paper we formulated a simple field-theoretic model for a melt of supramolecular diblock copolymers (SDC) in which end-functional A and B homopolymers can reversibly bond to form diblock copolymers. In this coarse-grained model, a free energy of bonding governs the tendency for dissimilar homopolymers to form a diblock copolymer. The formalism is developed in the grand canonical ensemble, the natural ensemble for reacting systems, and is fully consistent with the principles of chemical and reaction equilibrium. Unlike models for nonreacting two component polymer melts, both χN and N, where χ is the Flory interaction parameter and N is the length of the diblock copolymer, influence the phase behavior of the

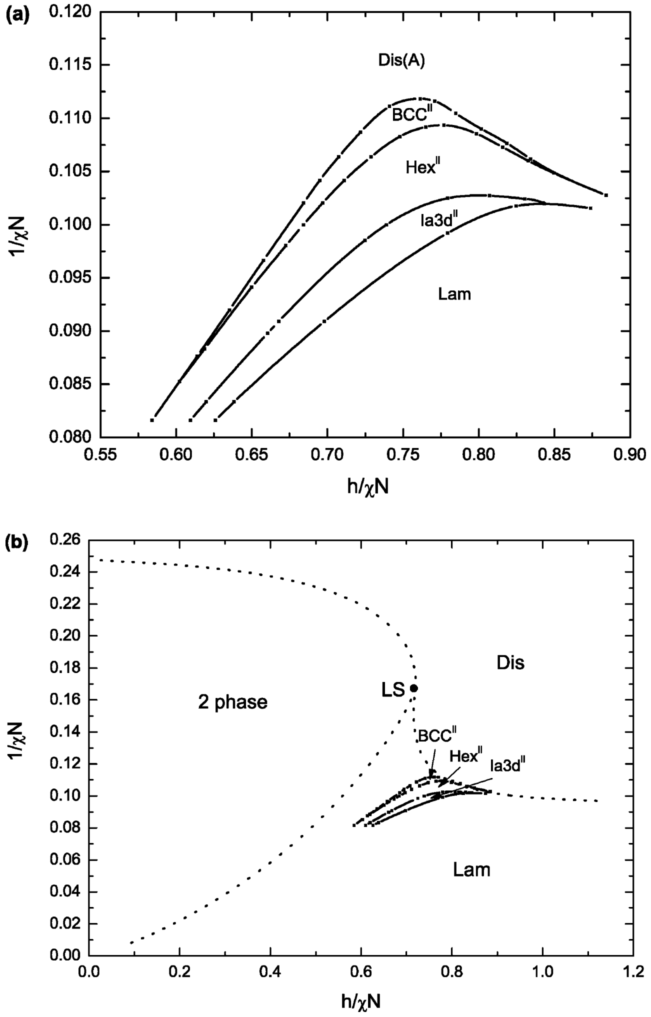

Figure 5. Mean-field phase diagram for an asymmetric supramolecular diblock copolymer at $z_A/z_B = 2.0$, $N_A = N_B$, and $N = 100$. Labeled phases are Dis (A-rich homogeneous phase), bcc^{II} (inverted bcc spheres), Hex^{II} (inverted hexagonal cylinders) $Ia3d^{II}$ (inverted bicontinuous double gyroid), Lam (lamellar). (a) Mean-field phase diagram in the coordinates $1/\chi N$ and $h/\chi N$. There is no Lifshitz point. (b) The phase diagram is superimposed on the symmetric phase diagram with $z_A/z_B = 1$ (dotted line) for comparison.

reacting system. The parameter N appears independently of χN in the formalism because one end segment of each homopolymer differs from the other segments in that it can react in a specific, hetero-complementary fashion to form diblocks. The theoretical approach is generalizable to other supramolecular architectures such as the three component graft copolymers discussed in the Introduction,[2] SDC with homo-complementary bonding in tandem with heterobonding, and supramolecular polymers that have more than one bonding group per polymer chain.

Using numerical self-consistent field theory, we presented a mean-field phase diagram for a system in which the A and B homopolymers have equal lengths and are present at equal volume fractions. There are several instances of re-entrant thermal behavior in which a phase disappears with decreasing temperature only to re-appear at a lower temperature. While previous studies of supramolecular diblock copolymer models have reported re-entrant behavior involving *homogeneous* disordered and macrophase separated phases, our numerical mean-field calculations also predict inhomogeneous re-entrant behavior involving a lamellar phase. Depending on the choice of parameters, the intermediate phase between the high and low-temperature lamellar phase is either disordered or macrophase separated. The topology of the phase diagram results from a delicate balance between bonding free energy, chemical incompatibility and the translational entropy loss upon forming diblock copolymers.

We are keenly interested in relating our theoretical work to experiments. While previous experiments have shown homogeneous re-entrant behavior in a supramolecular graft copolymer system[2] and thermal control of the microdomain period in supramolecular triblock copolymers,[27] we are unaware of any experiments that have systematically explored the phase diagram of SDC. The design of an experimental system for exploring the most interesting regions of the phase diagram requires a careful choice of chemistry for both the bonding groups as well as base polymer components. In the symmetric case of equal volume fractions and chain lengths, different regions of the phase diagram in Figure 3 can be accessed by fixing the chemistry of the bonding group and varying polymer length. Our formalism also provides a framework for the more tedious calculation of phase diagrams at fixed total volume fraction of the A species rather than an activity z_A. This type of temperature−volume fraction phase diagram can be accessed experimentally by simply blending the appropriate amounts of the two homopolymers. Finally, we note that experimental work on inhomogeneous supramolecular systems has shown the propensity for bonding groups to aggregate.[7] It may therefore be necessary to account for such effects by including additional interaction terms in our field-theoretic models.

Acknowledgment. This work was supported by the MRSEC Program of the National Science Foundation under Award No. DMR05-20415 and by funding provided to the Complex Fluids Design Consortium at UCSB by the Dow Chemical Company and Nestle Research Center. The authors are also pleased to acknowledge K. Katsov, E. Cochran, R. Elliott, V. Ginzburg, and K. Schaefer for useful discussions. E.H.F. thanks the Miller Institute at UC Berkeley for support during the preparation of this manuscript. Last, we thank a reviewer for the thoughtful comments that clarified our arguments in Appendix A.2.

A. Appendix

A.1. Derivation of Model. In this derivation, we use the subscript L to denote a quantity that applies to the A and B homopolymers and the AB diblock copolymer. For example, N_L denotes the length of the polymer for the three species. With the definitions given in section 2, the grand canonical partition function as a function of μ_A and μ_B, the chemical potential of the original A and B homopolymers respectively, is

$$\Xi(\mu_A, \mu_B, V, T) = \sum_{n_A^0,\, n_B^0=1}^{\infty} \frac{1}{n_A^0! n_B^0!} \sum_{n_{AB}=0}^{M(n_A^0, n_B^0)} \int \mathscr{D}\mathbf{R}_A \mathscr{D}\mathbf{R}_B \times D(n_{AB}; [\mathbf{R}_A, \mathbf{R}_B]) C(\{n_A^0, n_B^0\}, n_{AB}) \times \delta(\rho_0 - \hat{\rho}_A(\mathbf{r}) - \hat{\rho}_B(\mathbf{r})) \lambda_T^{-3(n_A^0 N_A + n_B^0 N_B)} \times e^{-U_0[\mathbf{R}_A, \mathbf{R}_B] - U_1[\mathbf{R}_A, \mathbf{R}_B] + \mu_A n_A^0 + \mu_B n_B^0 - F_b n_{AB}} \quad (24)$$

where $M(a, b)$ denotes the minimum of a and b, $\delta(\rho_0 - \hat{\rho}_A(\mathbf{r}) - \rho_B(\mathbf{r}))$ enforces incompressibility and

$$\mathscr{D}\mathbf{R}_A \mathscr{D}\mathbf{R}_B \equiv \prod_{i=1}^{n_A^0} \mathscr{D}\mathbf{R}_{iA} \prod_{j=1}^{n_B^0} \mathscr{D}\mathbf{R}_{jB} \quad (25)$$

denotes a functional integration over the space curves of the polymers. Also, $C(\{n_A^0, n_B^0\}, n_{AB})$ is a combinatorial factor

$$C(\{n_A{}^0, n_B{}^0\}, n_{AB}) = \frac{n_A{}^0!n_B{}^0!}{n_A!n_B!n_{AB}!} \tag{26}$$

that gives the number of ways in which $n_A{}^0$ and $n_B{}^0$ distinguishable homopolymers of species A and B can form n_{AB} indistinguishable diblock copolymers, and $D(n_{AB}; [\mathbf{R}_A,\mathbf{R}_B]) \equiv \prod_{i=1}^{n_{AB}} \delta(\mathbf{R}_{iA}(N_A) - \mathbf{R}_{iB}(N_B))$ stipulates that the first n_{AB} homopolymers of each species form diblock copolymers. We write the configurational integral for one possible arrangement of homopolymers into diblock copolymers and then multiply by $C(\{n_A{}^0, n_B{}^0\}, n_{AB})$ to account for all ways in which homopolymers can link together to form n_{AB} copolymers. In this derivation, it will be convenient to regularize the field theory and represent each space curve as a discrete set of beads connected by harmonic springs, known as the discrete Gaussian chain model.[14] Each functional integral $\mathscr{D}\mathbf{R}_{iK}$ for K = A, B becomes the product of N_K integrations over a position vector. If we assume each bead has the same mass, λ_T is the thermal wavelength that results from a one-dimensional momentum integration.

For any state with $n_A{}^0$ and $n_B{}^0$ original polymers, the chemical reaction to form a diblock copolymer implies $n_K{}^0 = n_K + n_{AB}$ where n_K is the number of free homopolymer for K = A, B. Then

$$e^{\mu_A n^0{}_A + \mu_B n_B{}^0} = e^{\mu_A n_A + \mu_B n_B + (\mu_A + \mu_B) n_{AB}} \tag{27}$$

gives $\mu_{AB} = \mu_A + \mu_B$, the criteria for chemical equilibrium. Moreover, the value of one chemical potential is arbitrary in an incompressible system. To show this, we first obtain

$$e^{\mu_A n_A{}^0 + \mu_B n_B{}^0} = e^{[\mu_A - \mu_B f/(1-f)] n_A{}^0} e^{\mu_B (n_A{}^0 f/(1-f) + n_B{}^0)} \tag{28}$$

by adding and subtracting $\mu_B n_A{}^0 f/(1 - f)$ from the argument of the exponential. Incompressibility implies that $e^{\mu_B(n^0{}_A f/(1-f) + n_B{}^0)} = e^{\mu_B \rho_0 V/N_B}$ is constant. Then only $\mu_A - \mu_B f/(1 - f)$ matters in calculating averages in the grand canonical ensemble, and we are free to choose a convenient value of μ_B that simplifies our formulas.

To make the partition function in eq 24 more manageable, we first note the equivalence of the following two summations

$$\sum_{n_A{}^0, n_B{}^0 = 0}^{\infty} \sum_{n_{AB}=0}^{M(n_A{}^0, n_B{}^0)} \leftrightarrow \sum_{n_A, n_B, n_{AB}=0}^{\infty} \tag{29}$$

which follows from the chemical reaction constraint $n_K{}^0 = n_K + n_{AB}$ for K = A, B. With the definition $\hat{\rho}_\pm(\mathbf{r}) \equiv \hat{\rho}_A(\mathbf{r}) \pm \hat{\rho}_B(\mathbf{r})$, we substitute $\hat{\rho}_A(\mathbf{r})\hat{\rho}_B(\mathbf{r}) = (\hat{\rho}_+(\mathbf{r})^2 - \hat{\rho}_-(\mathbf{r})^2)/4 = (\rho_0{}^2 - \hat{\rho}_-(\mathbf{r})^2)/4$ and the integral representation of a delta function $\delta(\rho_0 - \hat{\rho}_+(\mathbf{r})) = \int \mathscr{D}w_+ e^{i\int d\mathbf{r} w_+(\mathbf{r})(\rho_0 - \hat{\rho}_+(\mathbf{r}))}$ into eq 24 and perform a Hubbard–Stratonovich transformation to obtain

$$\Xi(\mu_A, \mu_B, V, T) = \sum_{n_A, n_B, n_{AB}=0}^{\infty} \frac{1}{n_A!n_B!n_{AB}!} \times \int \mathscr{D}w_\pm e^{-\rho_0\chi^{-1}\int w_-(\mathbf{r})^2 d\mathbf{r} + i\rho_0 \int w_+(\mathbf{r}) d\mathbf{r}} \left(e^{\mu_A} \frac{Q_A{}^0}{\lambda_T{}^{3N_A}} Q_A[w_\pm] \right)^{n_A} \times \left(e^{\mu_B} \frac{Q_B{}^0}{\lambda_T{}^{3N_B}} Q_B[w_\pm] \right)^{n_B} \left(e^{\mu_A + \mu_B - F_b} \frac{Q_{AB}{}^0}{\lambda_T{}^{3N}} Q_{AB}[w_\pm] \right)^{n_{AB}} \tag{30}$$

Here, $(n_A!n_B!n_{AB}!)^{-1}$ accounts for the indistinguishability of the polymers of each species, and $w_+(\mathbf{r})$ and $w_-(\mathbf{r})$ are the chemical potential fields conjugate to the $\hat{\rho}_+(\mathbf{r})$ and $\hat{\rho}_-(\mathbf{r})$ densities, respectively. Also, $Q_L[w_\pm]$ is the normalized single chain partition function in external fields (see eq 6 for Q_A), and $Q_L{}^0$ is the unnormalized single chain partition function in zero field. In the thermodynamics of chemical reactions, the chemical potential can be written $\mu_L = G_L{}^0 + \ln \bar{z}_L$ where $G_L{}^0$ is the Gibbs free energy of the standard state and $\bar{z}_L$ is the activity. For the homopolymers, we define $\bar{z}_K \equiv e^{\mu_K + \ln(Q_K{}^0/\lambda_T 3N_K)}$ for K = A, B since the standard state free energy $G_K{}^0 = -\ln(Q_K{}^0/\lambda_T{}^{3N_K})$ is the Gibbs free energy of a noninteracting one component polymer melt.[14] For the diblock copolymer, we define $\bar{z}_{AB} \equiv e^{\mu_{AB} + \ln(Q_{AB}{}^0/\lambda_T 3N_{AB}) - F_b}$ so that the standard state free energy $G_{AB}{}^0 = -\ln(Q_{AB}{}^0/\lambda_T{}^{3N_{AB}}) + F_b$ accounts for the microscopic details of bond formation. The quantity $Q_L{}^0/\lambda_T{}^{3N_L}$ is dimensionless since $Q_L{}^0$ is the product of N_L integrals over the position vectors of the monomers in the regularized field theory. For our model of supramolecular diblock copolymers, the chemical equilibrium condition $\mu_{AB} = \mu_A + \mu_B$ implies

$$\frac{\bar{z}_{AB}}{\bar{z}_A \bar{z}_B} = e^{-\Delta G^0} \tag{31}$$

the law of mass action where $\Delta G^0 \equiv G_{AB}{}^0 - G_A{}^0 - G_B{}^0$ is the free energy difference of the standard states.

Performing the summation over the number of polymers of each species in eq 30 leads to

$$\Xi(\mu_A, \mu_B, V, T) = \int \mathscr{D}w_\pm e^{-\mathscr{H}[w\pm]} \tag{32}$$

where

$$\mathscr{H}[w_\pm] = \rho_0\chi^{-1} \int w_-(\mathbf{r})^2 d\mathbf{r} - \rho_0 \int iw_+(\mathbf{r}) d\mathbf{r} - \bar{z}_A Q_A[w_\pm] - \bar{z}_B Q_B[w_\pm] - \bar{z}_{AB} Q_{AB}[w_\pm] \tag{33}$$

is the effective Hamiltonian. Each term in $\mathscr{H}[w_\pm]$ scales linearly with volume, since $\bar{z}_L$ is proportional to $Q_L{}^0$ which can be expressed as $Q_L{}^0 = V g_M{}^{N_L - 1}$ where g_M is a monomer volume independent of N. In the discrete bead–spring model, $g_M = (2\pi b^2/3)^{3/2}$. This implies that $(e^{\mu_L}/g_M)(g_M \lambda_T{}^{-3})^{N_L}$ is an activity with units of inverse volume, so then

$$z_L \equiv \frac{e^{\mu_L}}{g_M \rho_0} N (g_M \lambda_T{}^{-3})^{N_L} \tag{34}$$

is the dimensionless activity in units of ρ_0/N. We choose μ_B such that $z_B = 1$. With these new definitions, the law of mass action is

$$z_{AB} = z_A e^{-F_b} \frac{\rho_0 g_M}{N}, \tag{35}$$

and we absorb $\rho_0 g_M = e^{\ln \rho_0 g_M}$ into the definition of the bonding free energy. The effective Hamiltonian becomes

$$\mathscr{H}[w_\pm] = \rho_0\chi^{-1} \int w_-(\mathbf{r})^2 d\mathbf{r} - \rho_0 \int iw_+(\mathbf{r}) d\mathbf{r} - \frac{\rho_0 V}{N} \left(z_A Q_A[w_\pm] + Q_B[w_\pm] + z_A e^{-F_b} \frac{1}{N} Q_{AB}[w_\pm] \right) \tag{36}$$

After inserting the scaled vectors $\mathbf{x} = \mathbf{r}/R_{g0}{}^3$ and fields $W_\pm(\mathbf{x}) = N w_\pm(\mathbf{x})$ into eq 36, we obtain eq 5. This derivation is similar to a theoretical approach that two of us applied to equilibrium polymers with excluded volume.[28]

A.2. Bonding Free Energy. A more general free energy of bonding $F_b = -h + \ln q$ incorporates an entropy of bonding ln q. This entropy arises from the assumption that two bonding groups must be oriented as well as localized in space for bonding to occur. Then q is the extra number of orientational degrees of freedom associated with two bonding groups in the unbonded state compared to the bonded state. With this free energy, the effective diblock copolymer activity that multiplies $Q_{\mathrm{AB}}[W_{\pm}]$ in eq 5 can be written $z_{\mathrm{A}}\mathrm{e}^{h-\ln qN}$, so the explicit dependence on N can be viewed as part of an effective entropy of bonding.

We now relate this effective bonding free energy with the previous work of Angerman and ten Brinke.[12] In their Flory lattice model, each monomer that lies on a lattice site corresponds to l Kuhn segments of the actual polymer. This choice of l is arbitrary but must be large enough so that end-to-end distance of l Kuhn segments exhibits random walk statistics. For clarity, we define K_{A} as N from this previous work,[12] and K_{A} is the number of lattice monomers in an A homopolymer. Then K_{A} and l are artificial terms that arise due to the underlying lattice used in the derivation, but the physical quantity $K_{\mathrm{A}}l$ is the number of Kuhn segments comprising an A homopolymer, or N_{A} in the present work. Following Angerman and ten Brinke,[12] the dimensionless free energy change due to the loss of orientational and translational degrees of freedom in the bonding monomer is (ln ql). As a clever reviewer pointed out to us, the proper way to remove the artificial terms is

$$\ln ql = \ln qlK_{\mathrm{A}} - \ln K_{\mathrm{A}} = \ln qN_{\mathrm{A}} - \ln K_{\mathrm{A}} \qquad (37)$$

where $-\ln K_{\mathrm{A}}$ is the negative of a term from a different part of the free energy. For the total free energy, this analysis results in substituting (ln qN_{A}) for (ln q) in eq 23 of ref 12; the free energy remains independent of l and K_{A}. Hence, a Flory lattice treatment also implies a factor of N in an effective entropy of bonding. While this lattice treatment gives a term $\ln(qN/2)$, the factor of $^1/_2$ is inconsequential since we view q as a phenomenological parameter.

A recent experimental paper on supramolecular ABA triblock copolymers[27] employed a weak segregation theory[29] analogous to ref 12 to analyze their data. Their fitted value of $q \approx 10^6$ greatly differs from the previous expectation $q \approx 10^2$.[12] Assuming the weak segregation approximation is valid in understanding these experiments, the fitted value of q most likely reflects the product qN. This is consistent with the theoretical analysis in this work.

A.3. Random Phase Approximation. To derive the random phase approximation for supramolecular diblock copolymers, we use a weak inhomogeneity expansion[14] in the fields $W_{\mathrm{A}}(\mathbf{x}) \equiv E(\mathbf{x}) - P(\mathbf{x})$ and $W_{\mathrm{B}}(\mathbf{x}) \equiv E(\mathbf{x}) + P(\mathbf{x})$ that act on the A and B species, respectively. If we write the fields as $W_{\mathrm{I}}(\mathbf{x}) \equiv \bar{W}_{\mathrm{I}} + \Omega_{\mathrm{I}}(\mathbf{x})$ for I = A, B where $\bar{W}_{\mathrm{I}} = \bar{V}^{-1} \int W_{\mathrm{I}}(\mathbf{x})\,\mathrm{d}\mathbf{x}$ is the average value of the field and $\Omega_{\mathrm{I}}(\mathbf{x})$ represents the inhomogeneous contribution, then the density−density correlation function is

$$S_{\mathrm{IJ}}(\mathbf{x}, \mathbf{x}') = \frac{\rho_0 V}{N} N^2 \left(z_{\mathrm{A}} \frac{\delta^2 Q_{\mathrm{A}}[W_{\mathrm{A}}]}{\delta\Omega_{\mathrm{I}}(\mathbf{x})\delta\Omega_{\mathrm{J}}(\mathbf{x})} + \frac{\delta^2 Q_{\mathrm{B}}[W_{\mathrm{B}}]}{\delta\Omega_{\mathrm{I}}(\mathbf{x})\delta\Omega_{\mathrm{J}}(\mathbf{x})} + z_{\mathrm{A}}\mathrm{e}^{-F_{\mathrm{b}}-\ln N} \frac{\delta^2 Q_{\mathrm{AB}}[W_{\mathrm{A}}, W_{\mathrm{B}}]}{\delta\Omega_{\mathrm{I}}(\mathbf{x})\delta\Omega_{\mathrm{J}}(\mathbf{x})} \right)$$

where I and J can be A or B. The functional derivatives are evaluated to zeroth order in the fields Ω_{A} and Ω_{B}; in Fourier space, this gives

$$S_{\mathrm{AA}}(x) = z_{\mathrm{A}}\mathrm{e}^{-\bar{W}_{\mathrm{A}}f} Ng(x, f) + z_{\mathrm{A}}\mathrm{e}^{-F_{\mathrm{b}}-\ln N-\bar{W}_{\mathrm{A}}f-\bar{W}_{\mathrm{B}}(1-f)} Ng(x, f) \qquad (38)$$

$$S_{\mathrm{BB}}(x) = \mathrm{e}^{-\bar{W}_{\mathrm{B}}(1-f)} Ng(x, 1-f) + z_{\mathrm{A}}\mathrm{e}^{-F_{\mathrm{b}}-\ln N-\bar{W}_{\mathrm{A}}f-\bar{W}_{\mathrm{B}}(1-f)} Ng(x, 1-f) \qquad (39)$$

$$S_{\mathrm{AB}}(x) = z_{\mathrm{A}}\mathrm{e}^{-F_{\mathrm{b}}-\ln N-\bar{W}_{\mathrm{A}}f-\bar{W}_{\mathrm{B}}(1-f)}\, N\frac{1}{2}\Big(g(x, 1) - g(x, f) - g(x, 1-f)\Big) \qquad (40)$$

where the Debye function is

$$g(x, f) = \frac{2}{x^2}(fx - 1 + \mathrm{e}^{-fx}) \qquad (41)$$

and $x \equiv \mathbf{q}^2 R_{\mathrm{g0}}{}^2$. From the work of Leibler,[24] the second-order vertex function for a polymer system with two species is

$$\gamma_2(x) = \frac{S(x)}{W(x)} - 2\chi \qquad (42)$$

where

$$S(x) = S_{\mathrm{AA}}(x) + 2S_{\mathrm{AB}}(x) + S_{\mathrm{BB}}(x) \qquad (43)$$

$$W(x) = S_{\mathrm{AA}}(x)S_{\mathrm{BB}}(x) - S_{\mathrm{AB}}(x)^2. \qquad (44)$$

The conditions $\gamma_2(0) = 0$ and $\mathrm{d}\gamma_2(0)/\mathrm{d}x = 0$ give the location of the Lifshitz point. For $f = 0.5$ and $z_{\mathrm{A}} = 1$, it is straightforward to show that $\chi N = 6$, $\bar{W}_{\mathrm{A}} = \bar{W}_{\mathrm{B}} = \ln(9/4)$ and $F_{\mathrm{b}} = \ln(4/3N)$ corresponds to the Lifshitz point. Moreover, the comparison of eq 38 to 40 with eq 19a−c in previous work on ternary blends[17] shows that our analysis in section 3 gives the same result.

A.4. Variable Cell Shape Method. The cell shape in our simulation is defined by the 3 × 3 matrix **h** in which the columns are the vectors that define a parallelepiped cell.[14] Each component of the matrix **h** is a length in units of R_{g0}. For any given fields, the cell shape is updated according to

$$\mathbf{h}^{i+1} = \mathbf{h}^{i} - \lambda_h \mathbf{h}^{i}\Big(\mathbf{\Sigma}_{\mathrm{A}h}[W_{\mathrm{A}}, \mathbf{h}^{i}] + \mathbf{\Sigma}_{\mathrm{B}h}[W_{\mathrm{B}}, \mathbf{h}^{i}] + \mathbf{\Sigma}_{\mathrm{AB}}[W_{\mathrm{A}}, W_{\mathrm{B}}, \mathbf{h}^{i}]\Big)$$

where $\lambda_h > 0$ is a relaxation parameter and

$$\mathbf{\Sigma}_{\mathrm{A}h}[W_{\mathrm{A}}, \mathbf{g}] = 2z_{\mathrm{A}} \int \mathrm{d}\mathbf{X} \int_0^f \mathrm{d}t \times q(\mathbf{X}, t)\mathbf{g}^{-1}\nabla_{\mathbf{X}}\nabla_{\mathbf{X}}\,\mathbf{g}^{-1}q(\mathbf{X}, f-t)$$

$$\mathbf{\Sigma}_{\mathrm{B}h}[W_{\mathrm{B}}, \mathbf{g}] = 2 \int d\mathbf{X} \int_0^{1-f} \mathrm{d}t \times q^{\dagger}(\mathbf{X}, t)\mathbf{g}^{-1}\nabla_{\mathbf{X}}\nabla_{\mathbf{X}}\,\mathbf{g}^{-1}q^{\dagger}(\mathbf{X}, 1-f-t)$$

$$\mathbf{\Sigma}_c[W_{\mathrm{A}}, W_{\mathrm{B}}, \mathbf{g}] = 2z_{\mathrm{A}}\mathrm{e}^{-F_{\mathrm{b}}-\ln N} \times \int \mathrm{d}\mathbf{X} \int_0^1 \mathrm{d}t\, q(\mathbf{X}, t)\,\mathbf{g}^{-1}\nabla_{\mathbf{X}}\nabla_{\mathbf{X}}\,\mathbf{g}^{-1}q(\mathbf{X}, 1-t)$$

are the internal stresses of the A homopolymer, B homopolymer and diblock copolymer respectively in the grand canonical ensemble. Here, $\mathbf{g} \equiv \mathbf{h}^T\mathbf{h}$ and $\mathbf{X}$ is a position vector whose components lie in the interval [0, 1] such that the original Cartesian coordinates are $\mathbf{x} = \mathbf{h}\cdot\mathbf{X}$.

References and Notes

(1) Sijbesma, R. P.; Beijer, F. H.; Brunsveld, L.; Folmer, B. J. B.; Ky Hirschberg, J. H. K.; Lange, R. F. M.; Lowe, J. K. L.; Meijer, E. W.

Reversible polymers formed from self-complementary monomers using quadruple hydrogen bonding. *Science* **1997**, *278*, 1601.
(2) Ruokolainen, J.; Mäkinen, R.; Torkkeli, M.; Mäkelä, T.; Serimaa, R.; ten Brinke, G.; Ikkala, O. Switching supramolecular polymeric materials with multiple length scales. *Science* **1998**, *280*, 557−560.
(3) Gohy, Jean-Francois; Lohmeijer, Bas G. G.; Varshney, Sunil, K.; Décamps, Brigitte; Leroy, Eric; Boileau, Sylvie; Schubert, Ulrich, S. Stimuliresponsive aqueous micelles from an ABC metallo-supramolecular triblock copolymer. *Macromolecules* **2002**, *35*, 9748−9755.
(4) Xu, Jun; Fogleman, Elizabeth, A.; Craig, Stephen, L. Structure and properties of DNA-based reversible polymers. *Macromolecules* **2004**, *37*, 1863−1870.
(5) Castellano, Ronald, K.; Rudkevich, Dmitry, M.; Rebek, Julius, Jr. Polycaps: Reversibly formed polymeric capsules. *Proc. Natl. Acad. Sci. U.S.A.* **1997**, *94*, 7132−7137.
(6) Hofmeier, Harald; Schubert, Ulrich, S. Combination of orthgonal supramolecular interactions in polymeric architectures. *Chem. Commun.* **2005**, 2423−2432.
(7) Yamauchi, Koji; Lizotte, Jeremy, R.; Hercules, David, M.; Vergne, Matthew, J.; Long, Timothy, E. Combination of microphase separation and terminal multiple hydrogen bonding in novel macromolecules. *J. Am. Chem. Soc.* **2002**, *124*, 8599−8604.
(8) Tanaka, Fumihiko; Ishida, Masahiko; Matsuyama, Akihiko Theory of microphase formation in reversibly associating block copolymer blends. *Macromolecules* **1991**, *24*, 5582−5589.
(9) Tanaka, Fumihiko; Ishida, Masahiko Microphase formation in mixtures of associating polymers. *Macromolecules* **1997**, *30*, 1836−1844.
(10) Huh, J.; ten Brinke, G. Micro- and macrophase separation in blends of reversibly associating one-end-functionalized polymers. *J. Chem. Phys.* **1998**, *109*, 789−797.
(11) Huh, J.; Ikkala, O.; ten Brinke, G. Correlation hole effect in comblike copolymer systems obtained by hydrogen bonding between homopolymers and end-functionalized oligomers. *Macromolecules* **1997**, *30*, 1828−1835.
(12) Angerman, Hindrik Jan; ten Brinke, Gerrit Weak segregation theory of microphase separation in associating binary homopolymer blends. *Macromolecules* **1999**, *32*, 6813−6820.
(13) Fredrickson, Glenn, H.; Ganesan, Venkat; Drolet, Francois Fieldtheoretic computer simulation methods for polymers and complex fluids. *Macromolecules* **2002**, *35*, 16−39.
(14) Fredrickson, Glenn, H. *The Equilibrium Theory of Inhomogeneous Polymers*; Oxford University Press: Oxford, U.K., 2006.
(15) Matsen, M. W. Stabilizing new morphologies by blending homopolymer with diblock copolymer. *Phys. Rev. Lett.* **1995**, *74*, 4225−4228.
(16) Jannert, P. K.; Schick, M. Phase behavior of ternary homopolymer/diblock blends: Influence of relative chain lengths. *Macromolecules* **1997**, *30*, 137−144.
(17) Broseta, D.; Fredrickson, G. H. Phase equilibria in copolymer/homopolymer ternary blends: Molecular weight effects. *J. Chem. Phys.* **1990**, *93*, 2927−2938.
(18) Bates, F. S.; Maurer, W. W.; Lipic, P. M.; Hillmyer, M. A.; Almdal, K.; Mortensen, K.; Fredrickson, G. H.; Lodge, T. P. Polymeric bicontinuous microemulsions. *Phys. Rev. Lett.* **1997**, *79*, 849.
(19) Fredrickson, Glenn, H.; Bates, Frank, S. Design of bicontinuous polymeric microemulsions. *J. Polym. Sci., Part B: Polym. Phys.* **1997**, *35*, 2775−2786.
(20) Rasmussen, K. O.; Kalosakas, G. *J. Polym. Sci., Polym. Phys.* **2002**, *40*, 1777.
(21) Sides, S. W.; Fredrickson, G. H. Parallel algorithm for numerical selfconsistent field theory simulations of block copolymer structure. *Polymer* **2003**, *44*, 5859.
(22) Ceniceros, H. D.; Fredrickson, G. H. Numerical solution of polymer self-consistent field theory. *Multiscale Model. Simul.* **2004**, *2*, 452−474.
(23) Barrat, J. L.; Fredrickson, G. H.; Sides, S. W. Introducing variable cell shape methods in field theory simulations of polymers. *J. Phys. Chem. B* **2005**, *109*, 6694−6700.
(24) Leibler, L. Theory of microphase separation in block copolymers. *Macromolecules* **1980**, *13*, 1602−1617.
(25) Walker, James S.; Vause, Chester A. Reappearing phases. *Sci. Am.* **1987**, *256*, 98−105.
(26) Matsen, M. W.; Schick, M. Stable and unstable phases of a diblock copolymer melt. *Phys. Rev. Lett.* **1994**, *72*, 2660−2663.
(27) Huh, June; Park, Hui Joon; Kim, Keon Hyeong; Kim, Ki Hong; Park, Cheolmin; Jo, Won Ho. Giant thermal tunability of the lamellar spacing in block-copolymer-like supramolecules formed from binary-endfunctionalized polymer blends. *Adv. Mater.* **2006**, *18*, 624−629.
(28) Feng, Edward H.; Fredrickson, Glenn H. Confinement of equilibrium polymers: A field-theoretic model and mean-field solution. *Macromolecules* **2005**, *39*, 2364−2372.
(29) Huh, June; Jo, Won Ho. Theory on phase behavior of triblocklike supramolecules formed from reversibly associating end-functionalized polymer blends. *Macromolecules* **2004**, *37*, 3037−3048.

MA061653O